

УДК 539.12

RESULTS OF THE EXPERIMENT ON INVESTIGATION OF ^{76}Ge DOUBLE BETA DECAY

A. M. Bakalyarov, A. Ya. Balysh, S. T. Belyaev, V. I. Lebedev¹, S. V. Zhukov

Russian Research Centre «Kurchatov Institute», Moscow

On the termination of the Heidelberg–Moscow ^{76}Ge double beta decay experiment, the analysis of the data obtained from November 1995 to August 2001 is presented. The value of the half-life for two-neutrino double beta decay ($2\beta 2\nu$ mode) and limitation of the half-life for neutrinoless double beta decay ($2\beta 0\nu$ mode) are given.

Представлен анализ данных, набранных с ноября 1995 г. по август 2001 г., завершившего свою работу эксперимента «Гейдельберг–Москва», исследовавшего двойной бета-распад ^{76}Ge . Приведены полученные в результате данного анализа значения полупериода двухнейтринного двойного бета-распада ^{76}Ge и ограничение на полупериод безнейтринной моды этого распада.

1. EXPERIMENTAL SET-UP

High-purity germanium crystals, enriched with ^{76}Ge isotope up to 86%, are used as the main detecting elements. Five coaxial detectors with the total weight of 11.5 kg (125 moles in the active volume of detectors) are used. Each detector is located in a separate cryostat made of electrolytic copper with a low content of radioactive impurities. The quantity of other designed materials (iron, bronze, light material insulators) is minimized in order to reduce the feasible radioactive impurity contribution to the total background of the detectors.

The detectors are located in two separate shielded boxes. One of them, 270 mm thick, is made of electrolytic copper (detector No. 4), the other consists of two layers of lead. The inner one has 100 mm of high-purity LCD2-grade lead and the outer one has 200 mm of low-background Boliden lead (detectors Nos. 1, 2, 3, 5). Each set-up is coated with stainless steel casing. Non-radioactive pure nitrogen was blown through casings to reduce radon emanation contribution. To reduce neutron background the casing with detectors Nos. 1, 2, 3, 5 was coated with borated polyethylene and two anticoincidence plates of plastic scintillator were located over the casing in order to reduce muon component. The set-up is located in the Gran Sasso underground laboratory. The depth of 3500 m of water equivalent of the laboratory reduces influence of the cosmic rays on background conditions of the experiment.

The electronics and the system of data collection allow one to record each event which includes the number (or numbers) of acting detector, the amplitude and pulse shape, as well as anticoincidence veto. For details see [1]. The experimental data obtained within the period from November 1995 to August 2001 (200 days after the last detector started working in the set-up) are used in this work. In terms of the active volume for all the five detectors the statistical significance is equal to 50.5 kg · y.

¹E-mail: lebedev@polyn.kiae.ru

2. BACKGROUND MODEL

For correct interpretation of the data it is necessary to construct a model, which is the most suitable for the background conditions of the experiment. Varying the value and location of the background sources, one can reach the best agreement between the model and experimental spectrum. The uniform distribution of radioactive impurities in each material was the only a priori condition.

Response functions of detectors to products of decay of all isotopes of uranium and thorium radioactive chains were computed with the help of Monte Carlo method (GEANT3-2.1). Gamma quanta, electrons and bremsstrahlung, accompanying beta decay, were taken into account in the simulation. The response functions for other background sources, such as ^{40}K , ^{60}Co , ^{137}Cs , ^{134}Cs , ^{207}Bi , ^{125}Sb , ^{54}Mn , ^{65}Zn , were reliably identified by characteristic lines. In addition, the bremsstrahlung spectra of ^{210}Bi , as well as spectra of ^{60}Co , ^{68}Ga , ^{77}Ge , $\text{Sr} + ^{90}\text{Yt}$ and some other isotopes, presented as small impurities in germanium crystals, were included in computation. These impurities can contribute to total background, though without creating characteristic peaks, which identify them. The contribution of neutrons to background spectrum was computed as well. Consideration of surface contamination was also of importance, the α peaks of ^{210}Po , which are vividly seen in spectra of detectors Nos. 4, 5 stand for that possibility. The high-energy part of the spectrum is well described by α particles of Th and U radioactive chains (Fig. 1). The peaks are shifted to the left by 80–100 keV and have asymmetric shapes. All this shows that α sources are located on the surface of the crystals. The spectrum calculated with the assumption that α particles are passing through the dead zone in the detector well is in good agreement with observation. It is quite evident that products of uranium and thorium chains are close to the surface of the crystals, and that was also taken into account when constructing the background model.

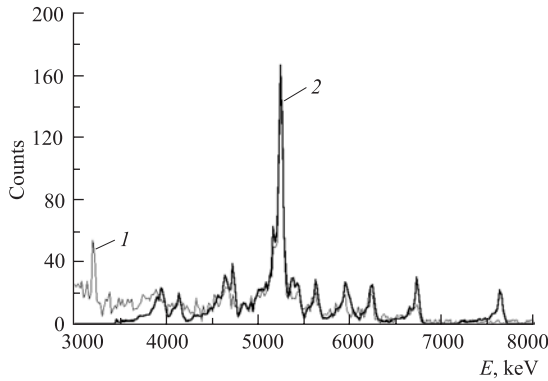


Fig. 1. Sum of spectra of all the five detectors in high-energy range, summarized in intervals of 20 keV. Curve 1 is experimental spectrum; curve 2 is simulated spectrum of α particles of thorium and uranium radioactive chains, which are in equilibrium with decay products. The shape of the spectrum was computed from the shape of experimental α spectrum of ^{210}Po

2.1. A Few Technical Details. Each time a supposed source of radioactive contamination was uniformly distributed in the volume (surface) of construction materials of the detectors and shielding. Contribution of each isotope was computed separately. Only information about the quantity of detected events in well-identified peaks was used. Search for minimum of function

$$F_{\min} = \sum_{i=1}^i \sum_{j=1}^j (x_{ij}(\text{sim}) - x_{ij}(\text{exp}))^2 \sigma_{ij}^2(\text{exp}) \quad (1)$$

for all the five detectors simultaneously was the criterion for correct description of spectrum, where i is the number of the detector; j is the number of the peak; $x(\text{sim})$ and $x(\text{exp})$ are areas of simulated and experimental peaks, and $\sigma(\text{exp})$ is statistical error in the area of experimental peak. The square of computed peak $x(\text{sim})$ is determined as a sum of all materials contributions

$$x(\text{sim}) = \sum_{n=1}^n x_n, \quad (2)$$

with n being a number of simulated parameters (materials). This method allows one to locate isotopes that have several peaks in spectrum (at least two peaks) with high accuracy. To locate isotopes with one peak in spectrum (^{137}Cs , ^{40}K) or without peaks (^{210}Pb), we used additional information, which we got from preliminary experiments (before 1995), when detectors worked incompletely assembled or inside individual shielding. Particularly using this method, we found a cesium spot on the inner surface of lead shielding, which explains relatively high background of cesium in detector No. 5.

Finally, contributions of separate isotopes computed before were considered as constants, but isotopes whose presence in germanium itself is possible and also the $2\beta 2\nu$ mode were varied separately for each detector. Bremsstrahlung of ^{210}Bi being present in lead shielding varied for detectors Nos. 1, 2, 3, 5 jointly.

The procedure of fitting was repeated many times for various low boundaries from which fitting started (low boundary varied from 200 to 1800 keV).

As a result of this fitting procedure, a constrained range of the most probable localization parameters for background sources was found. Uranium and thorium radioactive chains as well as cobalt and potassium in different combinations and the $2\beta 2\nu$ mode varied simultaneously. As a result of these fittings, the half-life for the $2\beta 2\nu$ mode of ^{76}Ge was calculated:

$$T_{1/2}(2\beta 2\nu) = (1.78 \pm 0.01 \text{ (stat.)}_{-0.09}^{+0.07} \text{ (syst.)}) \cdot 10^{21} \text{ y (68\% C.L.).} \quad (3)$$

The systematic error is mostly determined by inaccurate localization of background sources and also includes uncertainty in determination of active volume and degree of enrichment of germanium. Figure 2 gives the $2\beta 2\nu$ mode spectrum of ^{76}Ge decay.

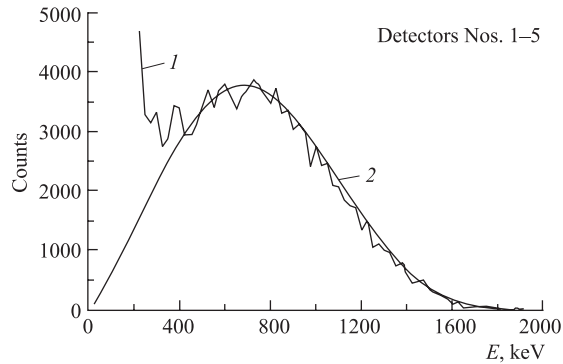


Fig. 2. Summarized spectrum of five detectors, integrated in 25 keV. Curve 1 is a difference between experimental data and simulated background; curve 2 is a computed value of half-life for the two-neutrino mode

2.2. Analysis of the Spectrum in the Range of the $2\beta 0\nu$ Mode. The suggested model allows one to describe the background in the neutrinoless beta decay region (see Fig. 3). The

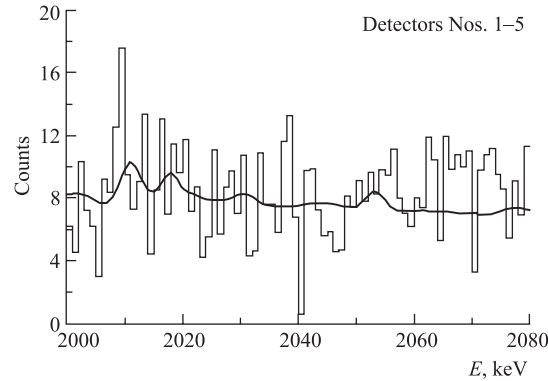


Fig. 3. The histogram is experimental data; smooth curve is a computed background

model describes around 90% of experimental data in the 2000–2080 keV region (in the 2000–2060 keV region it describes $\sim 98\%$). The important circumstance is that the background is practically constant in this region under investigation (the summarized quantity of events in three peaks of ^{214}Bi is less than 5% from the total background).

3. RELIABILITY OF EXPERIMENTAL DATA

Estimation of reliability of the experimental data was carried out in parallel with the calculation described above. The aim was to find out short-lived components and test the apparatus stability.

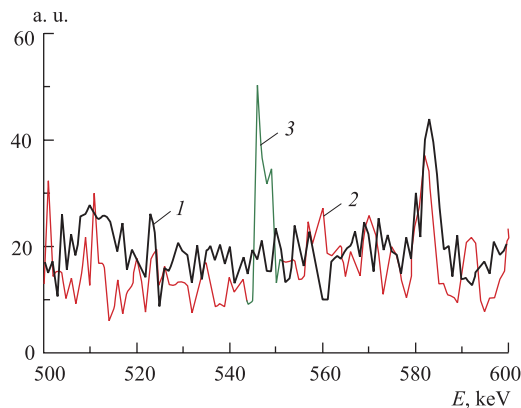


Fig. 4. Curve 1 corresponds to runs without underthreshold pulses (detector No.4); curve 2 corresponds to runs with underthreshold pulses (3 is unidentified peak). Spectra are normalized by time

apparatus stability. To make sure that all statistics corresponds to Poisson distribution and apparatus works correctly, the experimental data was randomly divided into several samples, and their spectra were compared. In particular, this analysis showed significant variations in time of ^{214}Bi and ^{214}Pb peaks, which stands for noticeable contribution to the background from ^{226}Rn inside the shielding. At the same time we found a number of peaks that could not be identified; their intensity changed arbitrarily for different detectors from sample to sample. They were better seen in the spectra of detector No.4. More careful analysis showed that those peaks appeared in the runs where there were pulses under discriminator threshold («underlevel» or underthreshold) and did not appear if there were no such pulses. In Fig. 4 one of such peaks is shown. Figure 5 shows characteristic amplitude spectra of one of the detectors (No.5) in the range below threshold of discrimination. The spectra

of detector No.4. More careful analysis showed that those peaks appeared in the runs where there were pulses under discriminator threshold («underlevel» or underthreshold) and did not appear if there were no such pulses. In Fig. 4 one of such peaks is shown. Figure 5 shows characteristic amplitude spectra of one of the detectors (No.5) in the range below threshold of discrimination. The spectra

were not normalized and their sum corresponds to full time of measurements with this detector. Pulses which occur lower than the discriminator threshold (dashed curve) are vividly seen. The runs with such pulses were tagged as «underlevel».

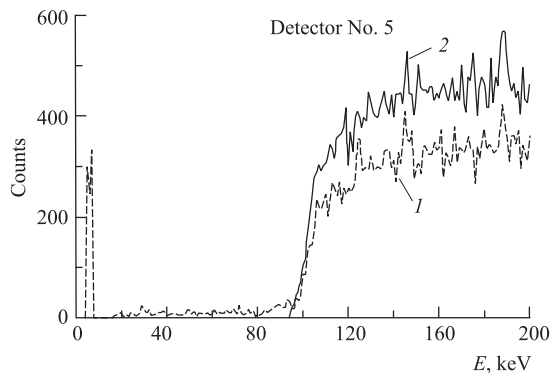


Fig. 5. Amplitude spectra in the low-energy range of detector No. 5. Curve 1 corresponds to runs with underthreshold pulses («underlevel»); curve 2 corresponds to runs without underthreshold pulses

The origin of the underthreshold pulses and false peaks cannot be disclosed without special control experiments. As a matter of fact, since underthreshold pulses did not occur in all runs, their quantity is quite small (1–3 per 100 events, typical for run of separate detector) and they were out of main energy range, we could not take them into consideration. But the fact that unidentified peaks appear (with the lower probability also in other detectors and in different regions) required more precise investigation of the experimental spectra, in order to analyze the influence of those events on evaluation of the physical result.

For this purpose, the set of the experimental data was divided into two subsets with underthreshold events and without them. Afterwards for each of the subsets (normalized by the total statistics) the calculation of the two-neutrino mode half-life was performed using the procedure described above. The spectra of the 2ν mode for these subsets, normalized by the time of measurement, are shown in Fig. 6. Two curves are in good agreement and the numerical difference might be taken into account as systematic error.

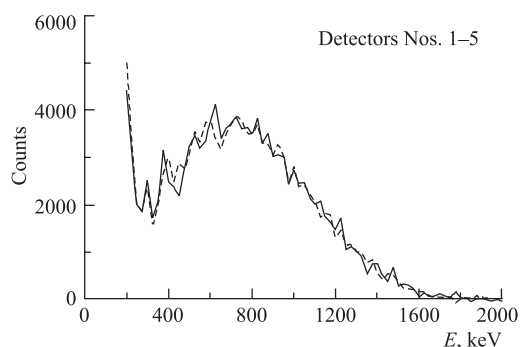


Fig. 6. Comparison of the two computed spectra of the 2ν mode. The spectrum without «underlevel» pulses is given as solid curve, and the spectrum with the «underlevel» pulses is given with dashed curve

The neutrinoless decay mode with its characteristic peak requires more specific analysis. All isotopes, which could get a peak in the energy range 2036–2042 keV, were investigated with great accuracy. It was shown that none of them could be responsible for appearance of peak in that energy range. It was decided to compare spectra with underthreshold events with spectra without such events. Statistical significance of those two sets is comparable.

Since false peaks do not appear in all runs with underthreshold events, a general view of spectra is close enough. But in some energy ranges the difference is rather visible. Figure 7

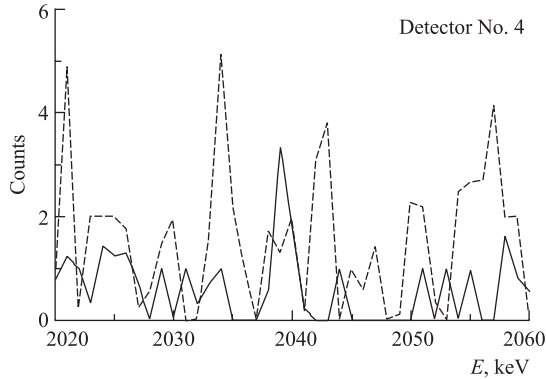


Fig. 7. Solid curve corresponds to runs without the underthreshold events, dashed curve corresponds to runs with the underthreshold events

illustrates comparison between two discussed sets for detector No.4 (it is located in individual shielding). Analogous comparison of spectra for neutrinoless double beta decay region from detectors Nos. 1, 2, 3, 5 seems to be of more interest. Two summarized in the 2039 keV energy range spectra of detectors Nos. 1, 2, 3, 5 with and without the underthreshold events are shown in Fig. 8. Looking at this figure, one can doubt that peak of 2039 keV has physical nature. Treatment of this part of the spectrum might be carried out by means of «Bayesian method», used in [2], where the experimental spectrum in 19 keV interval with the center at 2039 keV was considered as a sum of constant background and one Gaussian with determined energy resolution.

Algorithm permits one to get probability density function of Gaussian admission in the whole spectrum. The outcome of this procedure with the same energy window as in [2] shows that the peak appears in «underlevel» runs and it does not appear where there are no underthreshold events.

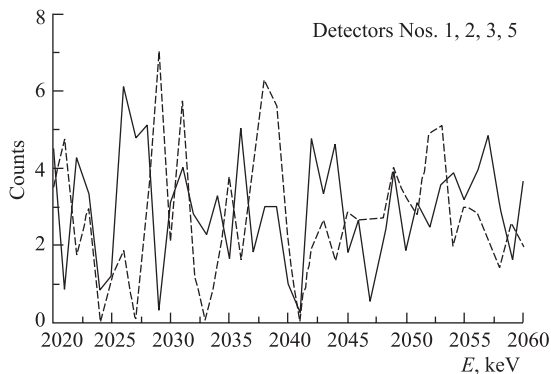


Fig. 8. Solid curve corresponds to runs without underthreshold events; dashed curve corresponds to runs with underthreshold events. The data are not normalized; the time of collecting statistics for assembling of four detectors is approximately equal (47% for «underlevel» runs and 53% without those runs)

It is necessary to note that this peak is obtained only in detectors Nos. 3, 5. Spectrum of the total statistics of detectors Nos. 1, 2 and runs of detectors Nos. 3, 5 without «underlevel» runs are presented in Fig. 9. Statistical significance of this set corresponds to 70% of the total statistics. This figure clearly testifies against the presence of the peak. The treatment of the spectrum by Bayesian algorithm suggested in [2] just confirms this result.

It is interesting to compare the integrals of Gaussian peaks, computed with the «Bayesian algorithm» (best value) for the three following sets. The integrated number of events for detectors Nos. 3, 5 («underlevel» set) is 14.3; for detectors Nos. 1, 2, 3, 5 («underlevel» set) it is 12.4 and finally it is 11.5 for the total sum of events from detectors Nos. 1, 2, 3, and 5. The Gaussian contribution does not grow, while the total number of events changes from 43 to 104.

One might argue that the peak seen in 30% of statistics and not seen in 70% of it is just a trick of statistics. Evaluation shows that the probability of this case is less than 1%. We are forced to conclude that the appearance of this peak does not correspond to any decay line in this energy range and is not connected with statistics, and cannot be considered as any evidence of neutrinoless double beta decay.

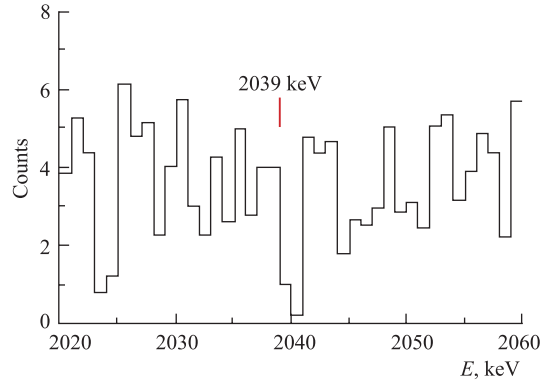


Fig. 9. The whole statistics of four assembled detectors without «underlevel» events of detectors Nos. 3, 5

CONCLUSIONS

Our result for the half-life of the $2\beta 2\nu$ mode is as follows:

$$T_{1/2}(2\beta 2\nu) = (1.78 \pm 0.01 \text{ (stat.)}_{-0.09}^{+0.07} \text{ (syst.1)} \pm 0.01 \text{ (syst.2)}) \cdot 10^{21} \text{ y (68\% C.L.)}, \quad (4)$$

where the difference between the two samples presented in Fig. 6 is included as an additional systematic error (syst.2).

Concerning the neutrinoless decay mode, it is necessary to stress the following: 1) an «evidence» of 2039 keV peak could be seen in the 3rd and 5th detectors' data and only in the runs with underthreshold pulses; 2) all the other runs of 4 assembled detectors (70% of statistics) do not give any evidence of 2039 keV peak. That is seen from Fig. 7 and confirmed from analysis with Bayesian algorithm.

To estimate half-life for neutrinoless decay mode, we have used all data in the 2000–2080 keV window. The total energy resolution in the 2039 keV range is (4.23 ± 0.14) keV, the background (without peaks of ^{214}Bi) is 0.163 counts/(kg · y · keV). The number of events expected in the interval of $\pm 3\sigma$ is 87 ± 3 , the quantity of events measured in the experimental spectrum is 89. Using the conservative procedure of estimation, as recommended in [3], we will get

$$T_{1/2}(2\beta 0\nu) \geq 1.55 \cdot 10^{25} \text{ y (90\% C.L.)}. \quad (5)$$

Consideration of the analysis of pulse shape can give additional opportunities to analyze experimental spectra. Since the method of pulse shape analysis with the help of neuron network has not been completely worked out yet, we do not perform the results of this analysis. Detailed comparative analysis for different pulse shape analysis methods and estimation of their sensitivity is performed in [4].

Acknowledgements. We thank all participants of NANP conference for useful discussions, especially M. V. Danilov, O. Ya. Zeldovich, and I. V. Kirpichnikov.

REFERENCES

1. *Gunther M. et al. (Heidelberg–Moscow Collab.) // Phys. Rev. D. 1997. V. 55. P. 54.*
2. *Klapdor-Kleingrothaus H. V. et al. // Mod. Phys. Lett. A. 2001. V. 16. P. 2409.*
3. *Feldman C. J., Cousins R. D. // Phys. Rev. D. 1998. V. 57. P. 3879.*
4. *Bakalyarov A. M. et al. hep-ex/0203017.*

Received on May 26, 2004.